Journal of Engineering Mathematics **27**: 73–87, 1993.

A two-dimensional bubble near a free surface

J.M. BOULTON-STONE
School of Mathematics and Statistics, University of Birmingham, Edgbaston, Birmingham, UK

Received 19 February 1992; accepted in revised form 5 June 1992

Abstract. A boundary integral technique is used in conjunction with a conformal map to examine the motion of a two-dimensional bubble near a free surface. For small times, the results are shown to compare well with a first-order perturbation expansion for the problem of the response of a free surface to a deeply submerged dipole. For a large bubble, far from the free surface the bubble deformation is found to agree with previous theoretical and experimental results for a two-dimensional bubble in an infinite fluid.

1. Introduction

This research, which examines at the motion of a two-dimensional bubble below a free gas/liquid interface, was motivated by experimental studies of cells in sparged bioreactors. It has been shown [1, 2] that there is a direct relationship between the presence of bubbles and cell death rate, and in particular that this death occurs primarily in a region close to the free surface [3]. In this paper, a two-dimensional bubble rising near a free surface is modeled using a boundary integral technique similar to those described by Boulton-Stone [4] for a bubble in an infinite fluid. The need to evaluate line integrals over the free surface in the discretised integral equations means that the Green's formula method given in [4] needs to be modified, this is done, as described in more detail below, by employing a conformal map.

There are many examples of numerical solutions to free surface problems in the literature. In an early use of the Green's formula boundary integral method, Longuet-Higgins and Cokelet [5] made a significant advance in the problem of the computation of breaking waves by being able, for the first time, to calculate the motion well after the interface had become vertical. Later, Baker, Meiron and Orszag [6] developed vortex and dipole distribution methods which they used to tackle the same problem. Using a modified version of their vortex method, Oguz and Prosperetti [7] obtained some beautiful pictures of the jet formed after a drop had impacted on a free surface. Boundary integral methods have also been used to calculate the motion of a vortex sheet and its effect on a free surface above (see for example [8, 9]).

The success of boundary integral methods in the field of cavitation bubbles is particularly noteworthy. Blake and Gibson [10] used a discrete ring-source distribution to approximately represent the cavitation bubble and adjacent free surface and thus follow the bubble's growth and collapse. They predicted motions that compared well with the experimental results given in the same paper. More recently, Blake, Taib and Doherty [11] used a full boundary integral technique to solve the same problem.

In order to solve for the motion of the bubble and free surface using a boundary integral method, it is necessary to discretise the integral equations into a set of algebraic equations. To do this, the relevant quantities such as position and potential have to be known at a finite number of points along the bounding surfaces of the solution domain. Thus it can be

appreciated that, as mentioned above, difficulties arise when one wishes to integrate over the free surface. For a bubble situated in a finite container, it is possible to integrate over the container walls and finite free surface, thus simplifying the task significantly. Another way of overcoming this problem, used in the axisymmetric case by Oguz and Prosperetti [12], is to integrate out for a finite radius and then match on a simple, first-order expansion for the potential and surface elevation valid for large distances from the bubble. If the velocities at the free surface are small then a linearised free surface boundary condition, namely that the potential vanishes there, may be used. This was one of the approaches taken by Blake and Gibson [10], and was achieved by using the appropriate image of the free-space Green's function in the $z = 0$ plane. For problems with periodic boundary conditions on the free surface, the integration can be simplified analytically by summing over all identical parts [6]. Alternatively they can be dealt with by using a conformal map, as in Longuet-Higgins and Cokelet [5], to transform all periodic parts onto a closed contour.

The method described here is a conformal mapping technique that maps the bubble beneath the initially flat free surface onto a bubble within the unit circle. The results obtained from the numerical solution are compared with a first-order perturbation expansion for the problem of a deeply submerged dipole.

2. Formulation of the problem

Unlike the study of the growth and collapse of cavitation bubbles where a bubble can just appear in the fluid near the free surface, in the case of gas bubbles in bioreactors, they rise some distance from a sparger before reacting with the interface. The two-dimensional bubble considered by Baker and Moore [13] breaks up after rising only a few bubble radii, and so a bubble that starts far away from the free surface will split up before getting close. Bearing this in mind, some of the example results for larger bubbles, given below, are for illustrative purposes only and are somewhat unphysical. However, for the case of much smaller bubbles, of sizes of the order of a millimeter, typical of those occurring in bioreactors, surface tension plays a significant role in keeping the bubble shape roughly elliptical, preventing jetting and breakup; thus the examples of a bubble with a radius of one millimeter are more realistic.

For the purposes of this study we assume any vorticity to be confined to thin boundary layers around the bubble and free surface so that the velocity field, $\mathbf{u}$, may be reasonably described by the gradient of a potential, ϕ. The total volume change for a bubble containing an ideal gas at fixed temperature, is given by

$$\frac{V}{V_0} \simeq (1 - \rho g \, \Delta y / p_\infty)^{-1} .$$

Taking p_∞ to be atmospheric pressure of the order of 10^6 dyn/cm^2, and since we are only interested in the motion of the bubble in the vicinity of the free surface, the total bubble translation, Δy, is only a few bubble radii, we find $\rho g \, \Delta y / p_\infty \ll 1$. This is in agreement with the experiments of Walters and Davidson [14] where the volume of a two-dimensional bubble is found to remain roughly fixed. Thus in the analysis that follows, we constrain the bubble volume to be constant.

For a kinematic boundary condition, we assume that there is no mass transport, thus if $\mathbf{r}(s, t)$ is a Lagrangian parameterisation of the free surface, then

$$\frac{\partial \mathbf{r}}{\partial t} = \nabla\phi(\mathbf{r}(s, t), t) . \tag{2.1}$$

The dynamic condition comes from Bernoulli's theorem

$$p_\infty = p + \frac{1}{2}\rho|\mathbf{u}|^2 + \rho\frac{\partial\phi}{\partial t} + \rho g y , \tag{2.2}$$

where p_∞ is the fluid pressure at infinity just below the free surface and ρ is the liquid density which is assumed to be much larger than that of the gas phase. Due to surface tension, T, we have the pressure balances

$$p = p_{\text{atm}} - T\kappa , \tag{2.3}$$

and

$$p = p_b(t) - T\kappa , \tag{2.4}$$

at the free surface and bubble respectively, where κ is the curvature at a point on the interface, p_{atm} is atmospheric pressure and $p_b(t)$ is the pressure inside the bubble. Since the gaseous contents of the bubble are much less dense than the liquid, p_b is assumed uniform throughout the bubble and the dynamics of the gas may be neglected. Evaluating (2.3) at a general point on the free surface and at infinity where the surface is assumed flat, eliminating p and p_∞ from (2.2) and using the substantial derivative, gives us an equation by which the evolution of the potentials of free surface particles may be followed through time. Scaling lengths with respect to the radius of the initially circular bubble, a, times with respect to $(a/g)^{1/2}$ and pressures with respect to $\rho g a$ gives us

$$\frac{D\phi}{Dt} = \frac{1}{2}|\mathbf{u}|^2 - y + \frac{4\kappa}{E_0} , \tag{2.5}$$

where the parameter $E_0 = 4\rho g a^2/T$ is the Eötvos number. If the bubble is initially at rest and γ_0 bubble radii below the surface, (2.2) and (2.4) evaluated at the bubble give us a similar expression for the potential on the bubble's surface,

$$\frac{D\phi}{Dt} = \frac{1}{2}|\mathbf{u}|^2 - (y + \gamma_0) + \frac{4}{E_0}(\kappa - 1) + p_b(0) - p_b(t) . \tag{2.6}$$

To eliminate p_∞, (2.2) and (2.4) have been evaluated at $t = 0$, $y = -h$ and use has been made of the Walters and Davidson [14] expression for the early potential on a bubble accelerating from rest.

The solution domain of the problem is the semi-infinite region of the complex z-plane below the free-surface, S, that is initially the real axis, bounded internally by the closed curve, B, representing the bubble. This region represents the area covered by the liquid and is denoted Ω_-. For convenience, write $C = S \cup B$. Normals to C are taken outwards from Ω_-.

The conformal mapping

$$\zeta = -\left(\frac{z + i\gamma_0}{z - i\gamma_0}\right) , \tag{2.7}$$

(where $\zeta = \xi + i\eta$) transforms Ω_- onto a finite region, $\tilde{\Omega}_-$, in the ζ-plane, bounded externally by the closed contour, $\tilde{S}$, initially the unit circle centred on the origin, $\tilde{O}$, and internally by the image of the bubble, $\tilde{B}$.

In order to determine the value of the $p_b(0) - p_b(t)$ term of (2.6), we introduce the quantity, $k(t) = \int_0^t (p_b(t') - p_b(0))dt'$, and on the boundaries, write

$$\tilde{f}(\zeta, t) = \tilde{\phi}(\zeta, t) + \begin{cases} k(t), & \zeta \in \tilde{B}, \\ 0, & \zeta \in \tilde{S}, \end{cases}$$

where $\tilde{\phi}$ is the potential in the ζ-plane.

By insisting that the bubble is to remain of constant volume, the problem becomes equivalent to a modified Dirichlet boundary value problem (see for example [15]). The constant, k, is determined by the side condition that the potential is the real part of a complex function, analytic in the solution domain and thus the flow field has no circulation or expansion.

We may now apply Green's formula to $\tilde{\phi}$, which we write for $\zeta \in \tilde{\Omega}_-$ as

$$\tilde{\phi}(\zeta) = \int_{\tilde{C}} \left(G(\zeta, \zeta') \frac{\partial \tilde{\phi}}{\partial n}(\zeta') - (\tilde{\phi}(\zeta') - \tilde{\phi}(\zeta)) \frac{\partial G}{\partial n'}(\zeta, \zeta') \right) \mathrm{d}S' - \tilde{\phi}(\zeta) \int_{\tilde{C}} \frac{\partial G}{\partial n'}(\zeta, \zeta') \, \mathrm{d}S', \tag{2.8}$$

where, $G(\zeta, \zeta') = -(1/2\pi) \log|\zeta' - \zeta|$ is the free-space Green's function and $\tilde{C} = \tilde{S} \cup \tilde{B}$. Since the last integral of (2.8) is equal to -1, taking the limit as $\zeta \to \tilde{C}$ and writing in terms of $\tilde{f}$ gives a first-kind Fredholm equation for $\partial\tilde{\phi}/\partial n$,

$$\int_{\tilde{C}} \left(G(\zeta, \zeta') \frac{\partial \tilde{\phi}}{\partial n}(\zeta') - (\tilde{f}(\zeta') - \tilde{f}(\zeta)) \frac{\partial G}{\partial n'}(\zeta, \zeta') \right) \mathrm{d}S' + \begin{cases} k, & \zeta \in \tilde{B}, \\ 0, & \zeta \in \tilde{S} \end{cases} = 0. \tag{2.9}$$

The side condition that the complex potential is analytic manifests itself, as suggested above, in the form of an integral requiring that the total flow out of the bubble vanishes, viz

$$\int_{\tilde{B}} \frac{\partial \tilde{\phi}}{\partial n} \, \mathrm{d}S = 0. \tag{2.10}$$

The dynamic conditions for $\tilde{f}$, from (2.5) and (2.6) become for the free surface

$$\frac{\mathrm{D}\tilde{f}}{\mathrm{D}t} = \frac{1}{2} |\mathbf{u}|^2 - y + \frac{4\kappa}{E_o}, \tag{2.11}$$

and for the bubble

$$\frac{\mathrm{D}\tilde{f}}{\mathrm{D}t} = \frac{1}{2} |\mathbf{u}|^2 - (y + \gamma_0) + \frac{4}{E_0}(\kappa - 1). \tag{2.12}$$

In order to update the position of the fluid particles taken on $\tilde{C}$, the velocities are required in the ζ-plane. For this, we use the identity

$$\frac{\mathrm{D}\zeta}{\mathrm{D}t} = \left| \frac{\mathrm{d}\zeta}{\mathrm{d}z} \right|^2 \left(\frac{\mathrm{d}\tilde{\Phi}}{\mathrm{d}\zeta} \right)^*, \tag{2.13}$$

where an asterisk denotes a complex conjugate and $\tilde{\Phi}$ the complex potential. Hence using (2.7) to evaluate the first factor of (2.13) and taking components, we see that the normal and tangential particle velocities in the ζ-plane are

$$\frac{1}{4\gamma_0^2}|\zeta+1|^4\frac{\partial\tilde{\phi}}{\partial n}, \text{ and } \frac{1}{4\gamma_0^2}|\zeta+1|^4\frac{\partial\tilde{\phi}}{\partial\tau} \tag{2.14}$$

respectively, where $\partial/\partial n$ and $\partial/\partial\tau$ represent derivatives taken normally and tangentially in the ζ-plane, in the sense $n = i\tau$.

In order to evaluate the $\frac{1}{2}|\mathbf{u}|^2$ term of the Bernoulli pressure condition, we use the relation

$$|\mathbf{u}|^2 = \frac{4\gamma_0^2}{|\zeta+1|^4}\left|\frac{D\zeta}{Dt}\right|^2. \tag{2.15}$$

The numerical method is covered in more detail in [4], but is briefly described below. Firstly the bubble and free surface are discretised in the ζ-plane using linear elements and N_B and N_S nodes respectively. Placing points on the free surface evenly spread according to arc length in the ζ-plane and points on the bubble according to arc length in the z-plane, ensures that resolution is not lost when plotting out the position of the free surface and bubble, whilst allowing accurate calculations. Initially, the free surface is taken to be the image of the x-axis and the bubble the image of the unit circle centered on $y = -\gamma_0$. As the fluid is initially at rest, we may take $\tilde{f} = 0$ at all nodes.

The boundary integral equations (2.9) and (2.10) are evaluated using a Gauss quadrature scheme, yielding a linear system which may be solved for $\partial\tilde{\phi}/\partial n$ using Gauss elimination. The derivatives of the potential in the normal and tangential directions can then be used together with (2.14) to move the surfaces through time. Similarly, (2.11) and (2.12) can be employed in conjunction with (2.15) to update $\tilde{f}$. The curvatures are evaluated by fitting quadratics to three adjacent points on the surfaces in the z-plane, and taking arc-length derivatives to give tangents and then curvatures. This '5-point' method gives reasonable results provided that there are not surface oscillations on the scale of the segment lengths, which may be avoided by using a sufficient number of nodes together with frequent application of the Longuet-Higgins and Cokelet [5] smoothing formula. To prevent points on the bubble and free surface becoming too irregularly spaced it is necessary to use a repositioning scheme frequently. An iterative trapezium rule is used for the time integrations.

3. Perturbation expansion

In order to approximate the effect on a free surface of a rising bubble, consider the problem of finding the free surface elevation as a function of time due to a dipole moving far below the surface. We may expect this to give reasonable agreement with the numerical result since for a bubble of constant volume, the dipole term is dominant in the far field.

Similar analytic studies have been undertaken before. For the problem of a submerged source or sink, Vanden Broeck, Schwartz and Tuck [16], developed a power series in the square of a Froude number for the free surface elevation. They did this by considering the steady Bernoulli equation, written in terms of inverse variables, evaluated at $\psi = 0$.

Havelock [17] studied the effect of placing a circular cylinder in a uniform stream, just below a free surface.

With the same scalings as in Section 2, assume that the dipole accelerates from rest from a point a distance $\gamma_0 = 1/\varepsilon$ below the free surface, for $\varepsilon \ll 1$ and let $\gamma(t) > 0$ be the distance of the dipole below the x-axis as a function of time. Re-defining Ω_- to be the semi-infinite region below the free surface, the problem can be formulated as follows. Laplace's equation must be satisfied by the potential everywhere except at the dipole, namely

$$\nabla^2\phi = 0\,, \text{ in } \Omega_-\backslash\{(0, -\gamma(t))\}\,, \tag{3.1}$$

with

$$\phi(\mathbf{r}) \sim -U(t)\,\frac{y+\gamma(t)}{x^2+(y+\gamma(t))^2}\,, \text{ as } \mathbf{r}\to(0,-\gamma(t))\,, \tag{3.2}$$

where $U(t) = -\mathrm{d}\gamma/\mathrm{d}t$ is the dipole's rise speed and $U(0) = 0$. Initially, the free surface, given by the curve $y = \eta(x, t)$, is flat and the fluid occupying Ω_- is stationary.

The first boundary condition is the usual kinematic condition, this time in the Eulerian form

$$\frac{\partial\eta}{\partial t} + \left.\frac{\partial\phi}{\partial x}\right|_{y=\eta}\frac{\partial\eta}{\partial x} = \left.\frac{\partial\phi}{\partial y}\right|_{y=\eta}. \tag{3.3}$$

If we assume that the curvatures on the free surface remain small, the pressures across this interface can be assumed to be continuous and the dynamic condition, similar to (2.5) is, in dimensionless variables,

$$\left(\frac{1}{2}|\nabla\phi|^2 + \frac{\partial\phi}{\partial t}\right)\Bigg|_{y=\eta} + \eta = 0\,. \tag{3.4}$$

Since $\gamma = O(\varepsilon^{-1})$, $(y+\gamma)/[x^2+(y+\gamma)^2] = O(\varepsilon)$, as $\varepsilon\to 0$ for fixed x and y, and so we expect to be able to expand the potential and free surface elevation in the form

$$\phi(x, y, t) = \varepsilon\phi_1(x, y, t) + \varepsilon^2\phi_2(x, y, t) + O(\varepsilon^3)\,. \tag{3.5}$$

$$\eta(x, t) = \varepsilon\eta_1(x, t) + \varepsilon^2\eta_2(x, t) + O(\varepsilon^3)\,, \tag{3.6}$$

with the first-order potential given by the solution to

$$\nabla^2\phi_1 = 0\,, \text{ in } \Omega_-\backslash\{(0, -\gamma(t))\}\,, \tag{3.7}$$

and

$$\phi_1(\mathbf{r}) \sim -\frac{U(t)}{\varepsilon}\,\frac{y+\gamma(t)}{x^2+(y+\gamma(t))^2}\,, \text{ as } \mathbf{r}\to(0,-\gamma(t))\,, \tag{3.8}$$

and higher orders satisfying

$$\nabla^2\phi_i = 0, \text{ in } \Omega_-,\ i \geq 2\,. \tag{3.9}$$

Since this is a free boundary perturbation problem, Taylor expand each of the terms in (3.5) about $y = 0$, and substitute for η as defined in (3.6). This gives

$$\phi(x, \eta, t) = \varepsilon\phi_1\Big|_{y=0} + \varepsilon^2\left(\eta_1 \frac{\partial\phi_1}{\partial y} + \phi_2\right)\Big|_{y=0} + O(\varepsilon^3)\,, \tag{3.10}$$

with similar expressions for $\partial\phi/\partial t$, $\partial\phi/\partial x$ and $\partial\phi/\partial y$ at the free surface. Substituting (3.6) and (3.10) into the kinematic and dynamic conditions (3.3) and (3.4), produces the first-order (linearised) boundary conditions

$$\frac{\partial\phi_1}{\partial t}\Big|_{y=0} + \eta_1 = 0\,, \tag{3.11}$$

and

$$\frac{\partial\eta_1}{\partial t} = \frac{\partial\phi_1}{\partial y}\Big|_{y=0}\,. \tag{3.12}$$

The second-order boundary conditions are given by

$$\left\{\left(\frac{\partial\phi_1}{\partial x}\right)^2 + \left(\frac{\partial\phi_1}{\partial y}\right)^2 + 2\left(\eta_1 \frac{\partial^2\phi_1}{\partial y\partial t} + \frac{\partial\phi_2}{\partial t}\right)\right\}\Big|_{y=0} + 2\eta_2 = 0\,,$$

and

$$\frac{\partial\eta_2}{\partial t} + \frac{\partial\phi_1}{\partial x}\Big|_{y=0}\frac{\partial\eta_1}{\partial x} = \eta_1 \frac{\partial^2\phi_1}{\partial y^2}\Big|_{y=0} + \frac{\partial\phi_2}{\partial y}\Big|_{y=0}\,,$$

but here, we restrict ourselves to solving only the first-order problem.

Combining equations (3.11) and (3.12) gives a condition for the first-order potential

$$\left(\frac{\partial^2\phi_1}{\partial t^2} + \frac{\partial\phi_1}{\partial y}\right)\Big|_{y=0} = 0\,. \tag{3.13}$$

To solve the first-order problem posed by equations (3.7), (3.8) and (3.13), apply a technique analogous to that used by Havelock [17] for a similar problem by writing ϕ_1 as the sum of a singular part,

$$\phi_S(x, y, t) = -\frac{U(t)}{\varepsilon}\left(\frac{y + \gamma(t)}{x^2 + (y + \gamma(t))^2} + \frac{y - \gamma(t)}{x^2 + (y - \gamma(t))^2}\right), \tag{3.14}$$

and an unknown harmonic part, ϕ_H. Note that the second term in (3.14) makes the analysis slightly simpler by anticipating the form of the final solution since, from (3.11), ϕ_S does not contribute to the surface elevation. A similar approach to this can be employed to find the response of the free surface to the fundamental singularity and hence determine the Green's function; see for example Wehausen and Laitone [18], where many surface wave problems are examined in detail.

Solving this problem for the harmonic potential, using integral transform methods, gives

$$\phi_H(x, y, t) = -2\int_0^t \frac{U(\tau)}{\varepsilon}\left(\int_0^\infty \sqrt{q}\,\exp(-q(\gamma(\tau) - y))\sin(\sqrt{q}(t - \tau))\cos(qx)\,\mathrm{d}q\right)\mathrm{d}\tau\,, \tag{3.15}$$

and thus (3.11) gives the surface elevation as

$$\varepsilon\eta_1(x, t) = 2\int_0^t U(\tau)\left(\int_0^\infty q\exp(-q\gamma(\tau))\cos(\sqrt{q}(t-\tau))\cos(qx)\,\mathrm{d}q\right)\mathrm{d}\tau\,. \tag{3.16}$$

To calculate the values of the integrals in (3.16), we first assume that, for small times, the bubble rises at a rate $U(t) = t$, and thus $\gamma(t) = 1/\varepsilon - t^2/2$ (see [14]). This is also justified if we assume the bubble to remain roughly circular, and use the fact that the added mass of a circular cylinder is equal to that of the displaced fluid.

4. Results and discussion

The boundary integral method outlined in Section 2 was used to solve the problem for various different Eötvos numbers, E_0, and initial distances from the free surface, γ_0. The first two figures show results for a bubble with $E_0 = 53$, equivalent to a 1 cm bubble in water. Figure 1 is a bubble that starts at rest with $\gamma_0 = 2$ bubble radii from the surface, whereas Fig. 2 is with $\gamma_0 = 10$. The latter case was introduced in order to test the method since at large distances from the free surface, a large bubble should move like a bubble in an infinite fluid without surface tension. Indeed, Fig. 2 is in close agreement with the findings of Baker and Moore [13] and Boulton-Stone [4], and qualitatively it matches the experimental results of Walters and Davidson [14]. The main difference, which can be clearly seen in the photographs of [14], is that the jet in the experiment widens out when it is further away from the top of the bubble. A careful comparison in [13] showed the computed jet speed to be greater, resulting in a slightly thinner, longer jet. They also found that the effect of surface tension did not remove this discrepancy, but possible reasons for differences were put forward. These relate to the fact that in the experiments, a two-dimensional bubble is approximated by injecting gas into the narrow gap between two sheets of glass which is filled with liquid. Thus, three-dimensional effects such as the formation of a meniscus or a thin film separating the bubble from the glass may be important.

The effect of the free surface for $\gamma_0 = 2$ is not very strong, but the jet broadens out earlier than in Fig. 2, as the flow around the bubble is slightly slower. This is due to gravity acting on the free surface thus preventing, to a certain extent, flow from above the bubble which is unhindered in the infinite fluid case.

Figure 3 is the corresponding time sequence for a bubble with $E_0 = 0.53$ and $\gamma_0 = 10$. Here, the surface tension effect is much larger and acts so as to keep the bubble almost elliptical, without any jet formation.

To calculate the pressure in the fluid, (2.2) was used in conjunction with the potentials at points on a grid in the z-plane which were evaluated for each equivalent ζ-plane position using

$$\tilde{\phi}(\zeta) = \int_{\tilde{C}}\left(G(\zeta, \zeta')\frac{\partial\tilde{\phi}}{\partial n}(\zeta') - (\tilde{f}(\zeta') - l(\zeta', t))\frac{\partial G}{\partial n'}(\zeta, \zeta')\right)\mathrm{d}S'\,,$$

where

$$l(\zeta, t) = \begin{cases} k(t)\,, & \zeta \in \tilde{B}\,, \\ 0\,, & \zeta \in \tilde{S}\,. \end{cases}$$

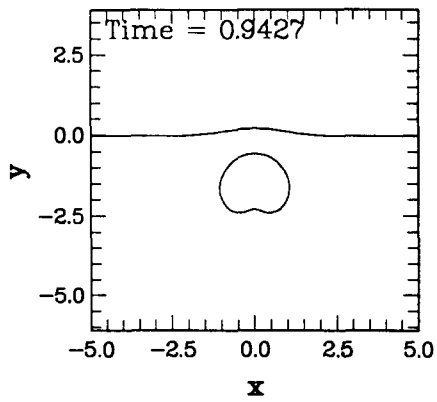

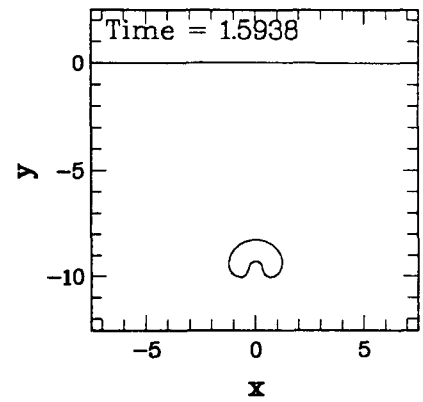

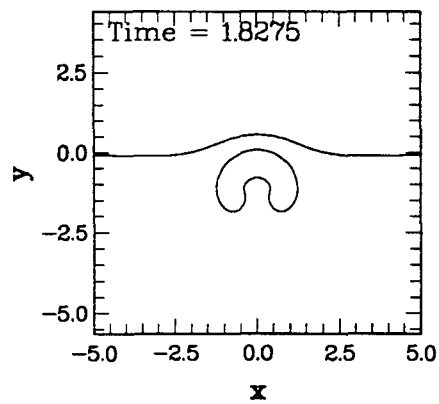

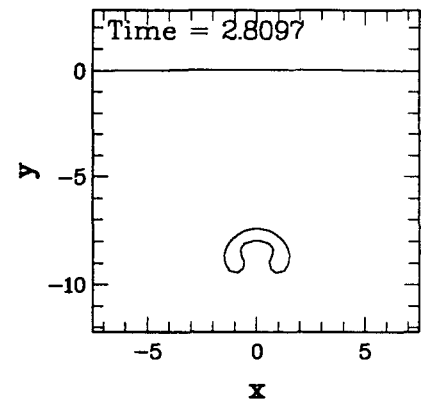

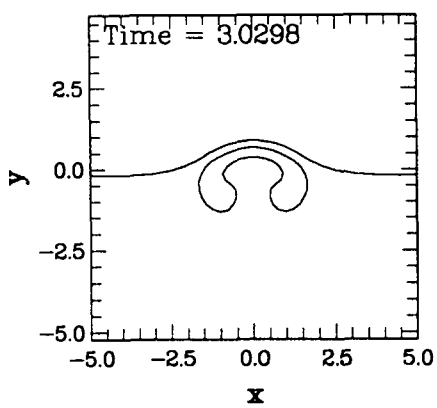

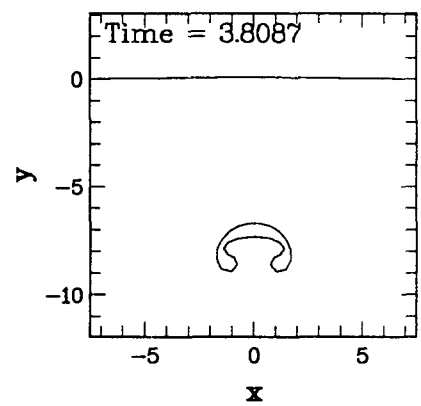

Fig. 1. The motion of a two-dimensional bubble near a free surface for the case $\gamma_0 = 2$, $E_0 = 53$. This is equivalent to a 1 cm air bubble in water. ($N_B = N_S = 50$ nodes were used.)

Fig. 2. As Fig. 1 but with $\gamma_0 = 10$. Compare with the case of a two-dimensional bubble in an infinite fluid.

In order to improve resolution around the bubble and free surface, the pressure at these surfaces was calculated explicitly using

$$p(\zeta, t) = p_\infty + \begin{cases} \mathrm{d}k/\mathrm{d}t - 4(\kappa - 1)/E_0 + \gamma\,, & \zeta \in \tilde{B}\,, \\ -4\kappa/E_0\,, & \zeta \in \tilde{S}\,. \end{cases}$$

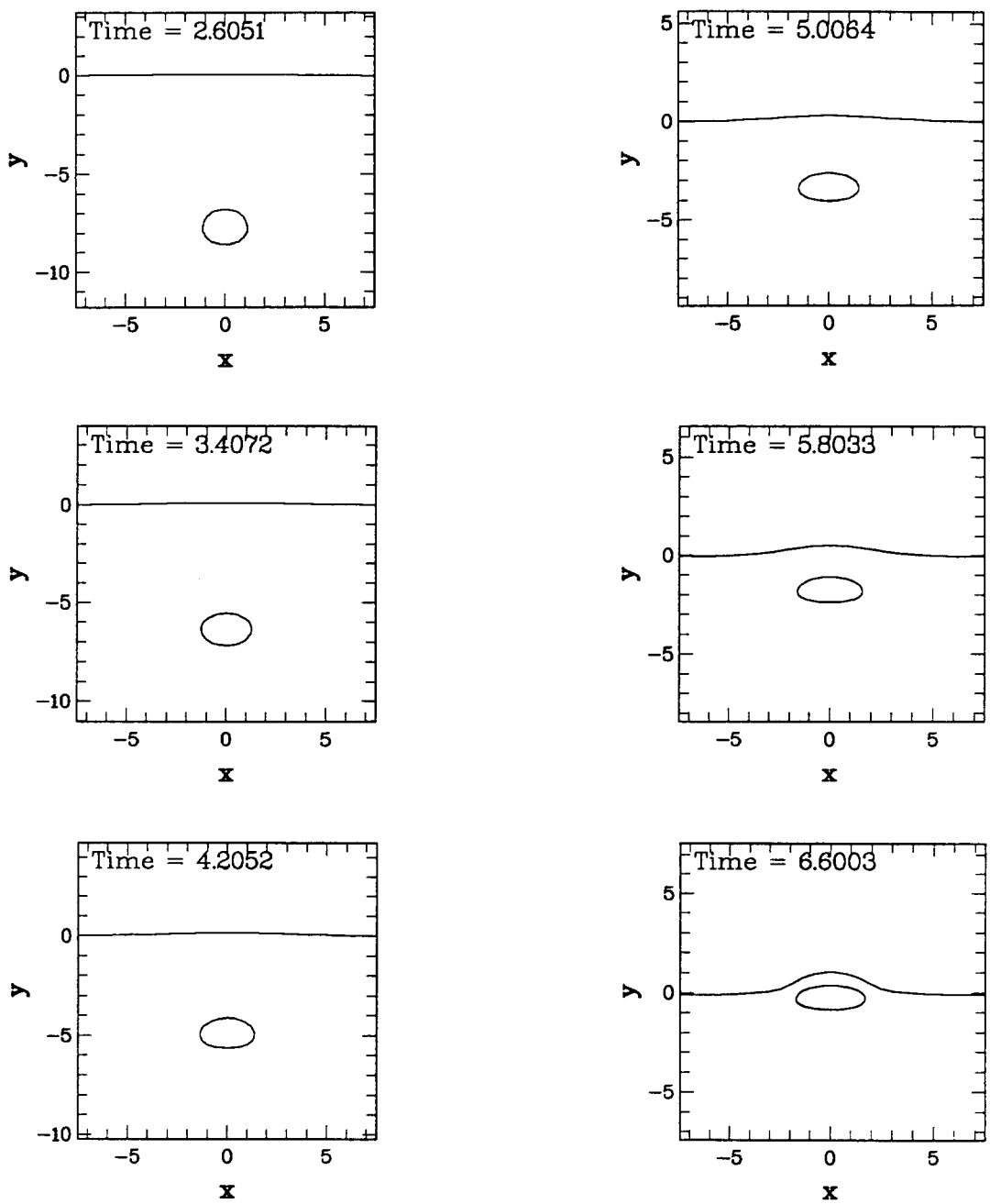

Fig. 3. Here the effect of surface tension for a small bubble is seen. In this example $\gamma_0 = 10$ and $E_0 = 0.53$, or a 1 mm air bubble in water.

Streamlines were calculated by using the stream function, given by

$$\tilde{\psi}(\zeta) = \int_{\tilde{C}} \left(-\theta(\zeta' - \zeta) \frac{\partial \tilde{\phi}}{\partial n}(\zeta') + (\tilde{f}(\zeta') - l(\zeta', t)) \frac{\partial G}{\partial \tau'}(\zeta, \zeta') \right) \mathrm{d}S' ,$$

where $2\pi\theta(\zeta' - \zeta)$ is the angle between $\zeta' - \zeta$ and the ξ-axis. Figure 4 shows pressure and

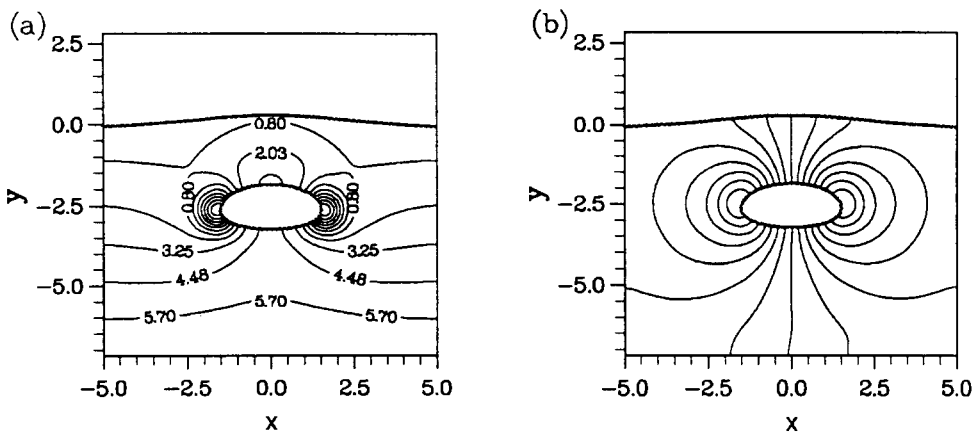

Fig. 4. Pressure contours (a) and streamlines (b) for the bubble of Fig. 3 at $t = 5.5$.

streamline plots corresponding to the bubble in Fig. 3 at time $t = 5.5$. The lower pressures around the sides of the bubble, as a result of faster flow than at the top, can be seen. To reach an equilibrium, the bubble has moved into an elliptical shape so that the curvatures at the sides allow for the correct jump between the fluid pressure and the uniform bubble pressure. It is also clear from the pressure plot that there is a higher pressure region directly above the bubble which acts to push the free surface up as the bubble approaches. The streamlines indicate that the free surface is moving up above the bubble and down and outwards to the left and right of the bubble.

In order to investigate the convergence of the solution of the discretised form of the integral equation (2.9) as the number of nodal points increases we consider an example problem where the exact solution is known. This problem is

$$\nabla^2\phi = 0\,, \text{ in } \Omega_-\,,$$

with Dirichlet boundary conditions

$$\phi = 0\,, \text{ on } S\,,$$

$$\phi = -\left\{ y + \gamma_0 + \frac{y - \gamma_0}{1 - 4y\gamma_0} \right\}, \text{ on } B\,,$$

where, as before, S is the free surface, taken here to be the x-axis, and B is the bubble, taken to be the unit circle centered at $(0, -\gamma_0)$. The exact solution is given by

$$\phi(x, y) = -\left\{ \frac{y + \gamma_0}{x^2 + (y + \gamma_0)^2} + \frac{y - \gamma_0}{x^2 + (y - \gamma_0)^2} \right\},$$

which is clearly just a dipole, representing the bubble's translation, together with its image in S. On the basis of the analysis in Section 3, equation (3.14) in particular, we would expect this to be typical of the type of boundary value problem solved by the numerical code when calculating the bubble motion, and hence it should give us a practical estimate for the rate-of-convergence.

To measure convergence, the normal derivative estimated on the transformed free surface by the boundary integral method with $N_S = N_B = N$ nodes, denoted $\tilde{\psi}_N$, is compared with that from the exact solution. The exact normal derivative in the z-plane is

$$\psi|_S \equiv \left.\frac{\partial \phi}{\partial n}\right|_S = \frac{4\gamma_0^2}{(x^2+\gamma_0^2)^2} - \frac{2}{x^2+\gamma_0^2},$$

and is related to that in the ζ-plane, $\tilde{\psi}$, by the expression

$$\tilde{\psi} = \left|\frac{dz}{d\zeta}\right| \psi .$$

The error is defined to be

$$E_N = \max_{i=1,\ldots,N} \{\tilde{\psi}_N(x_i) - \tilde{\psi}(x_i)\} .$$

Inspection of Fig. 5 shows that the error falls off as N^{-2}, as is the case for a corresponding second-kind integral equation using a piecewise linear collocation method (see for example Atkinson et al. [19]). It was found in [4] that the 1-norm condition numbers for the discretised first-kind formulation, such as the Green's formula method used here, are significantly larger than for second-kind vortex or dipole distribution methods. Thus small errors introduced at each time-step may be amplified faster using this method. A source of such errors is the integration of (2.11) and (2.12), particularly because of the difficulty involved in accurately differentiating the surface shape twice to find the curvatures. Indeed, it is the inclusion of surface tension that necessitates the use of smoothing.

Problems can occur when solving integral equations with weakly singular kernels if elements become very close to nodes on other parts of the surface. If this happens on parts of the surfaces where the distances between adjacent nodes are relatively large, so that few quadrature points are used, the integrals along the elements closest to the observation node will not be calculated accurately. In the context of problems considered in this paper, this typically occurs in the cases when a small, circular bubble gets very close to the free surface or when a large bubble has developed a jet which is about to pinch off smaller bubbles. We

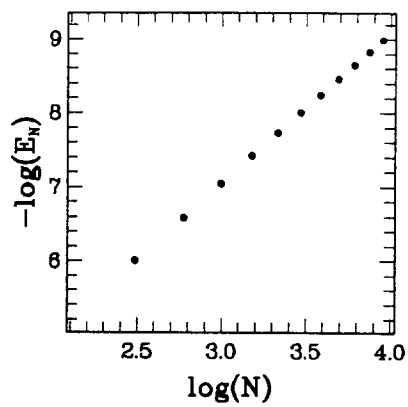

Fig. 5. The error in the normal derivative for a single inversion of the boundary integral equation, related to the number of nodes on each surface.

find that the problem tends to manifest itself by causing excessively large values for the normal derivatives as solutions to the integral equation. Here, we use the time-stepping method described in Boulton-Stone [4], where the time-step is chosen so as to restrict the maximum change in the potential to some prescribed value. From the dynamic conditions (2.11) and (2.12), we see that large velocities result in correspondingly large rates-of-change

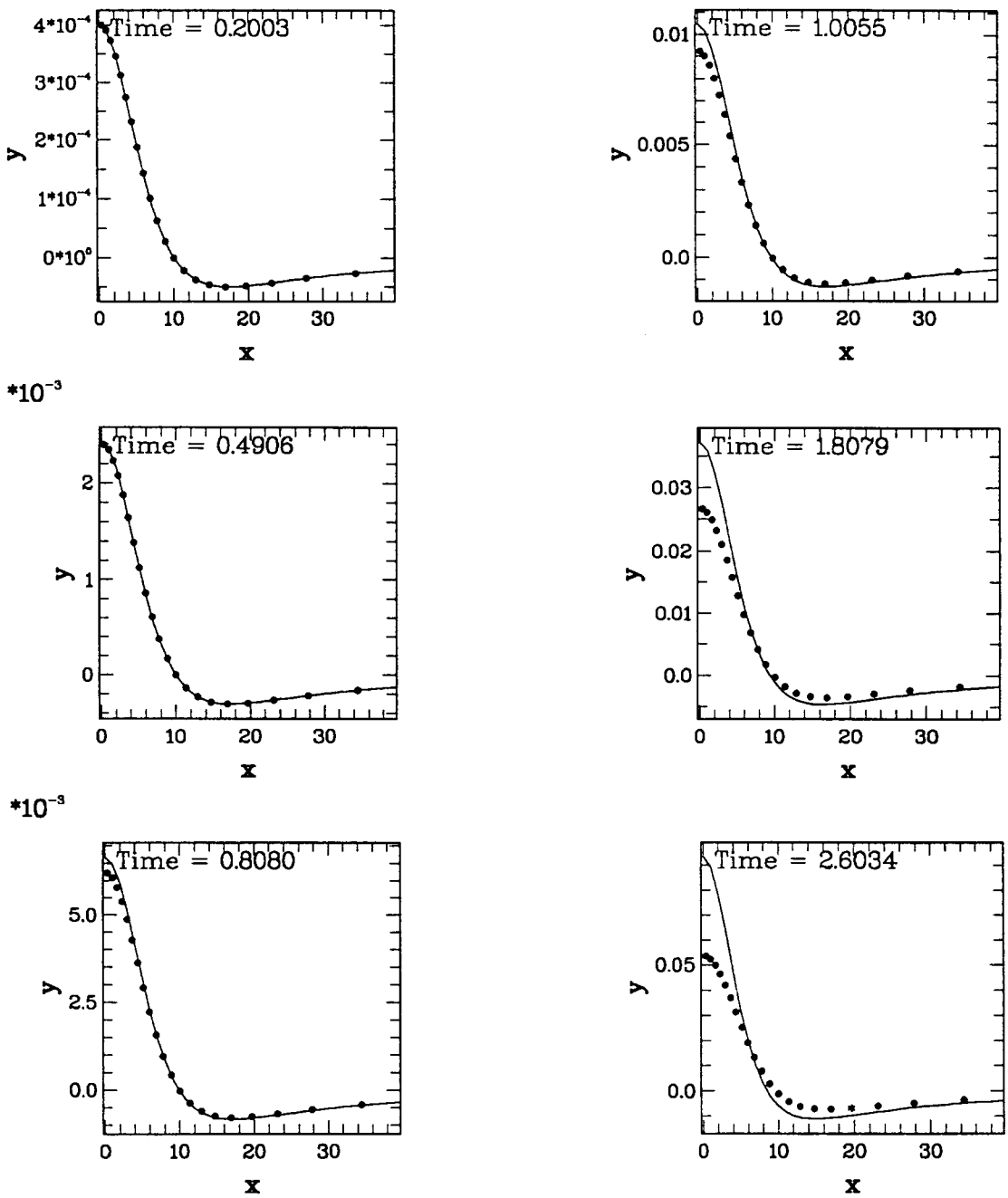

Fig. 6. Surface elevations for the numerical method of Section 3 (dotted lines), compared against those resulting from the linearised problem of a submerged dipole (solid lines), for the case $\gamma = 10$, $E_0 = 0.53$.

of potential, and thus a small time-step, eventually causing the calculation to grind to a halt. It is, however, important to note that for this particular application, these problems occurred in situations where one may expect viscous effects to be important, namely in the drainage of thin films. Thus the method will give good results to physical problems provided that small enough elements are used to ensure accuracy up to the point where the underlying assumptions of the model cease to be valid.

Figure 6 shows the results of the asymptotic expansion described in Section 3, for the case $\gamma_0 = 10$. The solid lines represent the surface elevations according to the analytic solution and the dotted lines the solution from the boundary integral method. The shapes of the analytic curves change very little through time suggesting that, for small times, the surface elevation given by (3.16) has the form $\eta \sim T(t)X(x)$ as $t \to 0$.

As expected, the curves compare best for small times when the bubble is further from the free surface and when the free surface elevation and velocity are small. As the bubble speeds up and moves closer, the comparison is less satisfactory.

There are several reasons for inaccuracy at later times. One factor that is bound to cause discrepancy is the fact that in the above analysis we assume that the bubble is represented by a dipole, and make no other attempt to ensure that the kinematic boundary conditions at the bubble are satisfied. Thus as the bubble deforms from circular or becomes much closer to the free surface the simple dipole model starts to break downs. Thus to get a better approximation, one could use the method of images to reinforce the boundary condition at the bubble on the assumption that it is a rigid cylinder as in [17]. One may also consider taking more terms in the asymptotic expansion. This should improve the comparison, however it should be emphasised that it would only yield a better approximation to the solution of the problem of a dipole's effect on a free surface and so could not hope to predict accurately the situation when the bubble becomes much closer to the surface, for the reason pointed out above. Another important factor causing inaccuracy is that in the analytic model described in Section 3, we assumed that the rise speed of the dipole was given by $U(t) = t$, where in fact the acceleration of the bubble is not quite constant. As the bubble draws closer to the surface, the fluid above the bubble is less mobile and thus cannot move around the bubble as easily, so that the acceleration is reduced. Thus the analytic result could be improved by using the actual rise speed as given by the numerical solution.

Acknowledgements

The author wishes to thank Professor J.R. Blake for his help and advice, the University of Birmingham Computing Service for use of their facilities and the Science and Engineering Research Council for financial support.

References

1. A. Handa, A.N. Emery and R.E. Spier, On the evaluation of gas-liquid interfacial effects on hybridoma viability in bubble column bioreactors. *Dev. Biol. Standard* 66 (1987) 241–253.
2. A. Handa, Gas-Liquid Interfacial Effects on the Growth of Hybridomas and Other Suspended Mammalian Cells. Ph.D. Thesis, University of Birmingham, U.K. (1986).
3. N. Kioukia, Physical and Chemical Factors Affecting Hybridoma Growth. M.Sc. Dissertation, University of Birmingham, U.K. (1990).

4. J.M. Boulton-Stone, A comparison of boundary integral methods for studying the motion of a two-dimensional bubble in an infinite fluid. To appear in *Comput. Methods Appl. Mech. Engrg.*
5. M.S. Longuet-Higgins and E.D. Cokelet, The deformation of steep surface waves on water. I. A numerical method of computation. *Proc. Roy. Soc. Lond. A* 350 (1976) 1–26.
6. G.R. Baker, D.I. Meiron and S.A. Orszag, Generalised vortex methods for free-surface flow problems. *J. Fluid Mech.* 123 (1982) 477–501.
7. H.N. Oguz and A. Prosperetti, Bubble entrainment by the impact of drops on liquid surfaces, *J. Fluid Mech.* 219 (1990) 143–179.
8. P.T. Fink and W.K. Soh, A new approach to roll-up calculations of vortex sheets. *Proc. Roy. Soc. Lond. A* 362 (1978) 195–209.
9. G. Tryggvason, Deformation of a free surface as a result of vortical flows. *Phys. Fluids* 31(5) (1988) 955–957.
10. J.R. Blake and D.C. Gibson, Growth and collapse of a vapour cavity near a free surface. *J. Fluid Mech.* 111 (1981) 123–140.
11. J.R. Blake, B.B. Taib and G. Doherty, Transient cavities near boundaries. Part II. Free Surface, *J. Fluid Mech.* 181 (1987) 197–212.
12. H.N. Oguz and A. Prosperetti, Surface tension effects in the contact of liquid surfaces. *J. Fluid Mech.* 203 (1989) 149–171.
13. G.R. Baker and D.W. Moore, The rise and distortion of a two-dimensional bubble in an inviscid liquid. *Phys. Fluids A* 1(9) (1989) 1451–1459.
14. J.K. Walters and J.F. Davidson, The initial motion of a gas bubble in an inviscid liquid. Part I. The two-dimensional bubble. *J. Fluid Mech.* 12 (1962) 408–417.
15. N.I. Muskhelishvili, *Singular Integral Equations*. Noordhoff (1953).
16. J.-M. Vanden Broeck, L.W. Schwartz and E.O. Tuck, Divergent low-Froude-number series expansions of nonlinear free-surface flow problems. *Proc. Roy. Soc. Lond. A* 361 (1978) 207–224.
17. T.H. Havelock, The method of images in some problems of surface waves. *Proc. Roy. Soc. Lond. A* 115 (1927) 268–280.
18. J.V. Wehausen and E.V. Laitone, Surface waves. *Handbuch der Physik* 9(3) (1960) 446–778.
19. K. Atkinson, I. Graham and I. Sloan, Piecewise continuous collocation for integral equations. *SIAM J. Numer. Anal.* 20(1) (1983) 172–186.